EpiMath Austria SEIR

A COVID-19 Compartment Model for Austria

Manu Eder, Joachim Hermisson, Michal Hledik
Christiane Hütter, Eugenia Iofinova, Rahul Pisupati
Jitka Polechova, Gemma Puixeu, Srdjan Sarikas
Benjamin Wölfl and Claudia Zimmermann*

August 30, 2020

Contents

*The authors are a diverse team of junior up to senior scientists based at several research institutions in and around Vienna, Austria.

1 Motivation

Compartment models are classical tools of mathematical epidemiology. They are used to analyze the spread of infectious diseases. For the current COVID-19 (coronavirus disease, WHO (2020b)) pandemic, variants of the basic SIR and SEIR (Susceptible - (Exposed) - Infectious - Removed) model have routinely been employed by modeling groups worldwide. However, the limits to the kinds of conclusions that can be drawn from such models are not always clear. Indeed, precise quantitative predictions of future infections or deaths in single countries that receive most attention in the media are usually outside of their scope. Rather, compartment models offer a deeper understanding of qualitative principles of infectious disease dynamics and insights into the range of possibilities – and impossibilities, given assumptions on key model parameters.

Below, we provide a detailed description of an SEIR model, with additional compartments - hospital and ICU wards, quarantine, recovery, and death - that describes the outcome of an epidemic that we have specifically adapted to the local outbreak in Austria. We describe several basic scenarios, discuss what can be learned from them and provide all necessary information for users to build their own scenarios and interpret the outcome.

2 Model

Our model is an extension of the well-studied SEIR model (Martcheva, 2015) without vital dynamics, i.e., the infectious disease spreads so fast that births and deaths unrelated to the epidemic can be neglected. It was initially loosely based on a COVID-19 simulation tool by Richard Neher et al. (University of Basel) (Noll et al., 2020). In the following sections, we first introduce the compartment structure of the model, including extensions of the basic SEIR structure to account for more detailed outcome dynamics and for population age structure. We then state the differential equations that define the dynamics and discuss the meaning of all model parameters.

2.1 Compartment structure

The basic SEIR model

All compartment models allocate the total population to a small number of compartments and assume that all individuals in the same compartment can be treated as identical with respect to the disease dynamics. The basic SEIR model has four such compartments. At the start of a new epidemic, almost all individuals are allocated to the susceptible (S) compartment. If an S-individual

meets an infectious (I) individual, he or she can get infected. In this case, the individual first moves from the S-compartment into the exposed (E) compartment. E-individuals have contracted the virus but are not yet infectious themselves, i.e., they are in the latency period. An E-individual turns into an I-individual after an (exponentially distributed) waiting time. From there, the individual transitions to the so-called "removed" (R) compartment, where s/he is no longer infectious, and also cannot be infected any more. For the disease dynamics, it does not matter whether individuals in the R-compartment are dead or whether they have recovered and are now permanently immune: both will not feed back on the dynamics of the S, E, and I-compartments. The basic SEIR model therefore does not distinguish these cases.

Of relevance to COVID-19, the basic SEIR model assumes a simple *black or white* scheme concerning immunity: One the one hand, there is no pre-existing immunity (or even partial immunity), on the other hand, there are no re-infections: once individuals are recovered, immunity is complete and permanent.

Outcome dynamics

As the disease outcome is of key interest in the real world, we extend the basic model and distinguish between Recovered (R) and Deceased (D) individuals. Note that the new R-class "Recovered" is really a sub-compartment of the R-compartment "Removed" of the basic model. For a more detailed description of the outcome dynamics, we include additional compartments: Quarantined (Q), Hospitalized (H), and intensive Care (C). Finally, the Recovered compartment is decomposed into a known/detected R^k and an unknown/undetected R^u compartment.

Infected individuals can either recover directly into R^u without ever being detected or they are detected, officially recorded and quarantined. Depending on the severity of the disease, these detected individuals progress to one of three quarantine compartments, Q, Q^h, or Q^c. While Q-individuals recover at home (and progress to R^k), Q^h-individuals require hospitalization (H) after some time and Q^c-individuals require intensive care (C). All H-individuals eventually recover into R^k, but C-individuals die with a certain probability (D) and are otherwise admitted to a normal hospital ward (H) to recover.

The dynamics of the H and C-compartments are of particular interest, since both have limited capacity due to a finite number of hospital and ICU beds, which should not be exceeded during the epidemic. Furthermore, at least partial time-series data exist for those compartments. Explicitly including them into the model can provide additional information about the various parameters.

Of course, the outcome dynamics of the model is a simplified view of the real-world dynamics. In particular, we assume that all deaths occur out of critical care and ignore potential hospital days of C-patients before they are admitted to critical care.

Age structure

The basic SEIR model assumes that all individuals in a compartment can be treated as equivalent. This is never true in reality, but with large compartments, individual differences can often be "averaged out". However, this is not possible for some key factors that influence the disease dynamics and the expected outcome. For COVID-19, the most important factor to determine outcome (and to some extent also transmission) is age. We have therefore added an explicit age structure to the model. Specifically, all compartments are subdivided into nine age groups in intervals of ten years, from the youngest ones (0-9 years) to the oldest (80 years and older). This follows international practice, as COVID-19 data (e.g., for ICU need) are often published for these age classes.

Compartment model summary

We can summarize the compartment structure and the flow chart of our model as follows:

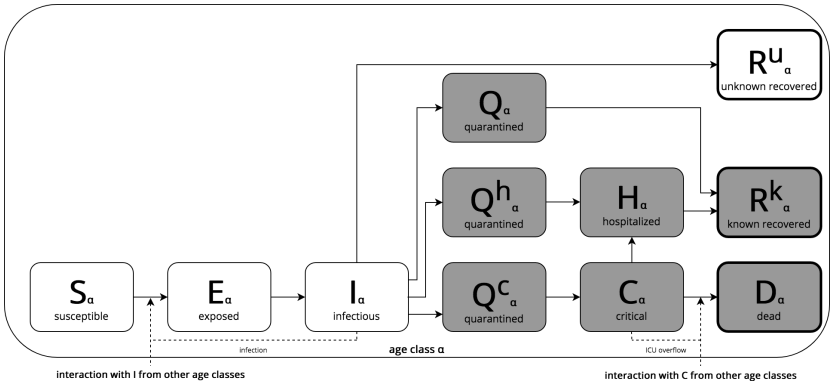

All compartments are sub-structured into nine age classes (index α). They contain the following classes of individuals:

- S_α: Susceptible individuals (not yet infected and not immune)
- E_α: Exposed individuals (infected, but non yet infectious, latency period)
- I_α: Infectious individuals (not in quarantine/hospital)
- R^u_α: Unknown recovered individuals (with permanent immunity)
- R^k_α: Known recovered individuals (with permanent immunity)
- Q_α: Quarantined individuals (usually with mild symptoms, i.e., recovering at home)
- Q^h_α: Quarantined individuals with severe symptoms that (eventually) require hospitalization.

- Q^c_α: Quarantined individuals with severe symptoms that (eventually) require critical care.
- H_α: Hospitalized individuals (with severe symptoms)
- C_α: Individuals in Critical care (occupying ICU beds)
- D_α: Deceased individuals

For all compartments, we will use the letter without index α to denote the total number of individuals across all age classes, i.e., $S = \sum_\alpha S_\alpha$ etc.

2.2 Dynamical equations and transition rates

We consider the dynamics of the various classes along time (in days), defined by the following system of ordinary differential equations (ODEs):

$$\frac{dS_\alpha}{dt} = \dot{S}_\alpha = -v_\alpha^{S\to E} \tag{1a}$$
$$\dot{E}_\alpha = v_\alpha^{S\to E} - v_\alpha^{E\to I} \tag{1b}$$
$$\dot{I}_\alpha = v_\alpha^{E\to I} - \left(v_\alpha^{I\to R^u} + v_\alpha^{I\to Q} + v_\alpha^{I\to Q^h} + v_\alpha^{I\to Q^c}\right) \tag{1c}$$
$$\dot{R}^u_\alpha = v_\alpha^{I\to R^u} \tag{1d}$$
$$\dot{R}^k_\alpha = v_\alpha^{Q\to R^k} + v_\alpha^{H\to R^k} \tag{1e}$$
$$\dot{Q}_\alpha = v_\alpha^{I\to Q} - v_\alpha^{Q\to R^k} \tag{1f}$$
$$\dot{Q^h}_\alpha = v_\alpha^{I\to Q^h} - v_\alpha^{Q^h\to H} \tag{1g}$$
$$\dot{Q^c}_\alpha = v_\alpha^{I\to Q^c} - v_\alpha^{Q^c\to C} \tag{1h}$$
$$\dot{H}_\alpha = v_\alpha^{Q^h\to H} + v_\alpha^{C\to H} - v_\alpha^{H\to R^k} \tag{1i}$$
$$\dot{C}_\alpha = v_\alpha^{Q^c\to C} - \left(v_\alpha^{C\to D} + v_\alpha^{C\to H}\right) \tag{1j}$$
$$\dot{D}_\alpha = v_\alpha^{C\to D}. \tag{1k}$$

The sum of individuals in each age class remains constant at all times,

$$S_\alpha + E_\alpha + I_\alpha + R^u_\alpha + R^k_\alpha + Q_\alpha + Q^h_\alpha + Q^c_\alpha + H_\alpha + C_\alpha + D_\alpha = N_\alpha. \tag{2}$$

We use the initial conditions,

$$\begin{aligned} E_\alpha(t_0) = R^u_\alpha(t_0) = R^k_\alpha(t_0) = Q_\alpha(t_0) = Q^h_\alpha(t_0) = Q^c_\alpha(t_0) \\ = H_\alpha(t_0) = C_\alpha(t_0) = D_\alpha(t_0) = 0, \end{aligned} \tag{3a}$$
$$S_\alpha(t_0) = N_\alpha - I_\alpha(t_0). \tag{3b}$$

Here, the initial number of infectious individuals, $I(t_0) = \sum_\alpha I_\alpha(t_0)$ and the start time t_0 are free parameters. These initial infections are distributed across age groups proportionally to their size, i.e., $I_\alpha(t_0) \propto N_\alpha$. Usually, $I_\alpha(t_0) \ll N_\alpha$.

The transition rates between compartments are defined as follows,

$$v_\alpha^{S\to E} = \frac{\beta_\alpha(t)}{T_i}\frac{S_\alpha(t)}{N}\sum_{\alpha'} I_{\alpha'}(t) \tag{4a}$$

$$v_\alpha^{E\to I} = \frac{1}{T_l}E_\alpha(t) \tag{4b}$$

$$v_\alpha^{I\to Q} = (1-h_\alpha)\frac{\delta(t)-\bar{h}}{1-\bar{h}}\frac{1}{T_i}I_\alpha(t) \tag{4c}$$

$$v_\alpha^{I\to Q^h} = h_\alpha(1-c_\alpha)\frac{1}{T_i}I_\alpha(t) \tag{4d}$$

$$v_\alpha^{I\to Q^c} = h_\alpha c_\alpha\frac{1}{T_i}I_\alpha(t) \tag{4e}$$

$$v_\alpha^{I\to R^u} = (1-h_\alpha)\frac{1-\delta(t)}{1-\bar{h}}\frac{1}{T_i}I_\alpha(t) \tag{4f}$$

$$v_\alpha^{Q\to R^k} = \frac{1}{T_q}Q \tag{4g}$$

$$v_\alpha^{Q^h\to H} = \frac{1}{T_{qh}}Q^h \tag{4h}$$

$$v_\alpha^{Q^c\to C} = \frac{1}{T_{qc}}Q^c \tag{4i}$$

$$v_\alpha^{H\to R^k} = \frac{1}{T_h}H_\alpha(t) \tag{4j}$$

$$v_\alpha^{C\to D} = \begin{cases} d_\alpha\frac{1}{T_c}C_\alpha(t), & \sum_\alpha C_\alpha \le C_{\mathrm{ICU}}, \\ d'_\alpha\frac{1}{T_c}C_\alpha(t), & \text{otherwise (ICU-overflow)} \end{cases} \tag{4k}$$

$$v_\alpha^{C\to H} = \begin{cases} (1-d_\alpha)\frac{1}{T_c}C_\alpha(t), & \sum_\alpha C_\alpha \le C_{\mathrm{ICU}}, \\ (1-d'_\alpha)\frac{1}{T_c}C_\alpha(t), & \text{otherwise (ICU-overflow).} \end{cases} \tag{4l}$$

Below, we describe the parameters of the model and our fitting procedure, and discuss results of the "EpiMath Austria SEIR" web application for several epidemic scenarios.

2.3 Definition of model parameters

Equations (4) describe how the transition rates of the dynamical model depend on a set of basic parameters for infection, recovery, and death. We now explain the meaning of these basic parameters in detail. In subsequent sections, we will describe how all parameters can be estimated from data.

Epidemiological parameters

A first set of parameters determines the basic epidemiological dynamics between compartments S, E, I, and the combined $R^u + R^k + Q + Q^h + Q^c + H + C + D$ compartment for the "removed" cases.

Reproduction number The key quantity to determine the course of an epidemic is the *effective reproduction number*,

$$\mathcal{R}_{\text{eff}}(t) = \sum_{\alpha} \beta_\alpha(t) \frac{S_\alpha(t)}{N} \tag{5a}$$

where

$$\beta_\alpha(t) = \mathcal{R}_0 \zeta_\alpha \big(1 - M(t)\big) \left(1 - \frac{\epsilon}{2} \Big(\cos\Big[2\pi \frac{t - t_{peak}}{365.25}\Big] + 1 \Big)\right). \tag{5b}$$

$\mathcal{R}_{\text{eff}}(t)$ is the average number of new infections caused by a single infected person throughout the infectious period (i.e., while in compartment I). For $\mathcal{R}_{\text{eff}}(t) > 1$, the number of infected individuals increases (the "epidemic grows"), while for $\mathcal{R}_{\text{eff}}(t) < 1$ it shrinks exponentially. The effective reproduction number is a composite, time-dependent quantity that summarizes several effects that are defined by the following parameters:

- The *basic reproduction number* $\mathcal{R}_0$ defines the average number of new infections per infected individual at the start of the epidemic, when all other individuals are still susceptible, and without any effects of mitigation or seasonality. It is also the maximal value that $\mathcal{R}_{\text{eff}}(t)$ can attain during the course of the epidemic.

- The *mitigation factor* $M(t) \in [0, 1]$ measures the relative reduction of $\mathcal{R}_0$ due to behavioral changes, both voluntary and imposed by governmental interventions. It thus summarizes the effects of many different measures such as increased hand washing, face masks, ban of large gatherings, social distancing, school closures, closures of shops and restaurants, etc. Our model implements the function $M(t)$ by a series of point mitigations, indicated by pairs of parameters for each change in mitigation: the date of the mitigation change t_j (with $j = 1, 2, 3, \dots$) and the new mitigation strength $M_j = M(t_j)$ for $t_j \le t < t_{j+1}$. (The last t_j is the simulation endpoint and appended automatically.)

- The *seasonal amplitude* ϵ and the *seasonal peak date* t_{peak} describe the mitigation of virus transmission due to seasonal forcing. Similar to the influenza (flu) virus, many human coronaviruses are known to have a marked seasonal transmission pattern with a winter peak (in temperate climates of the northern hemisphere; Monto et al. (2020)). In our model, seasonal forcing is included via a cosine modulation of the effective reproduction

number that is assumed independent of the mitigation factor $M(t)$. In contrast to the mitigation factor, which ought to suppress an imminent epidemic outbreak, the seasonal variability in transmission is independent of the virus outbreak dynamics. Seasonal effects are presumed to be driven both by behavioral changes (outdoor life in summer), and by the effect of the environment on the virus. Cool, dry environments have been associated with increased stability and transmissivity of coronaviruses (Kanzawa et al., 2020; Moriyama et al., 2020).

- Finally, the model includes an age-specific *isolation factor* ζ_α that allows for age-dependent differences in the social contact rate. This functionality is currently **not** implemented in the model.

Generation interval The so-called generation interval determines the time that elapses between the times of infection of two consecutive cases in the transmission chain. In the SEIR model, the distribution of the generation intervals follows from the times that each newly infected individual spends in the E and the I compartment. Both times are exponentially distributed, where

- the *mean latency time* T_l measures the average time spent in compartment E,
- the *average infectious period* T_i measures the average number of days an individual is infectious. Importantly, T_i summarizes the pre- and post-symptomatic infectious periods (until patients go to quarantine), as well as the infectious time of asymptomatic individuals.

The expected generation interval follows from these times as

$$T_{\mathrm{GI}} = T_l + T_i \,. \tag{6}$$

Relationship with daily increase in infections In the early stages of the epidemic, the number of infections in the E and I compartments grows approximately exponentially, increasing daily by the factor λ (see also Ma 2020):

$$\lambda = \exp \frac{\sqrt{(T_l + T_i)^2 + 4T_l T_i(\mathcal{R}_{\mathrm{eff}} - 1)} - (T_l + T_i)}{2T_l T_i}. \tag{7}$$

The system approaches this daily increase if, for a few days, the effective reproduction number $\mathcal{R}_{\mathrm{eff}}$ remains constant. That means that there are no changes in $\mathcal{R}_{\mathrm{eff}}$ due to mitigation or seasonality, and the majority of the population is still susceptible ($\sum_a S_a/N \approx 1$).

In practice, deviations from Eq. (7) are expected due to stochastic effects, as well as imported infections which can play a significant role when case numbers are low.

Disease outcome parameters

Once the individuals leave the I compartment, they are "removed" from the epidemiological dynamics. However, the outcome of the disease - recovery or death - can differ strongly. In the model, this is included via the Q, Q^h, Q^c, H, C, D, R^k and R^u compartments. The dynamics between these classes is regulated by an additional set of parameters.

Outcome waiting times All waiting times in the "outcome compartments" are exponentially distributed and assumed equal for all age classes (hence no age class index is used):

- T_h: mean time in H (hospital days)
- T_c: mean time in C (ICU days)
- T_q, T_{qh}, T_{qc}: mean time in Q, Q^h, or Q^c, respectively (quarantine days).

Outcome fractions The I and C compartments allow for transitions to two or more compartments. Outcome fractions determine the relative proportions that take either route.

Depending on the severity of the individual disease, patients from the I compartment can transition into H and subsequently to C and potentially to D. The probability for each step depends on age and is given by

- h_α: fraction of I individuals in age class α that go on to become hospitalized, either H or C (severe cases) and therefore progress to Q^h or Q^c.
- c_α: fraction of severe cases in age class α whose condition gets critical, C, and therefore require an ICU bed,
- d_α: fraction of C in age class α that become deceased, provided they receive ICU treatment. For patients who do not receive the required care due to ICU capacity overflow, d_α is inflated by a severity factor s. See more information about ICU overflow below.

For the C compartment, the remaining fraction $1 - d_\alpha$ progresses to a normal hospital ward H. For the I compartment, there are two further options (Q and R^u) depending on whether the case is diagnosed and officially recorded.

Detection ratio ($\delta(t)$) The parameter $\delta(t)$ is the time-dependent fraction of all infections that are detected and confirmed through testing and thus enter the official case records by the Austrian authorities. In the model, $\delta(t)$ controls the flow from the infectious (I) compartment: it is the fraction of individuals that proceed either to the hospital (H), or in mild/asymptomatic cases, to

quarantine (Q). The complementary fraction $1 - \delta(t)$ of infectious individuals remains unknown and proceeds to the recovered unknown (R^u) compartment.

Since all hospitalized COVID-19 patients are assumed to have detected infections, $\delta(t)$ must be at least as large as the overall hospitalization fraction,

$$\delta(t) \geq \bar{h} = \sum_\alpha N_\alpha h_\alpha / \sum_\alpha N_\alpha.$$

Before δ is applied, it is converted to a *detection ratio conditional on not being hospitalized*, $\delta' = \frac{\delta - \bar{h}}{1 - \bar{h}}$. The outflow from I_α is then divided into fractions $h_\alpha c_\alpha$, $h_\alpha(1 - c_\alpha)$, $(1 - h_\alpha)\delta'$, and $(1 - h_\alpha)(1 - \delta')$, which flow into Q^c_α, Q^h_α, Q_α and R^u_α, respectively.

In the current version of the model, the detection ratio $\delta(t)$ is not age-dependent. Age dependence in $\delta(t)$ would only change the age distribution within the Q, R^k and R^u compartments. Since all results presented in the application are sums over age categories, they are only sensitive to the overall $\delta(t)$.

Crucially, in reality, increased testing efforts will not only improve our knowledge about the outbreak, but also help contain it through targeted and early isolation of infectious individuals. This is currently **not** explicitly included in the model: the individuals who do or do not get detected spend (on average) the same time being infectious (I).

Infection fatality ratio (IFR) The infection fatality ratio refers to the probability of death from COVID-19 in the case of an infection. In terms of the transition rates of the model, the IFR of a randomly chosen infected person is

$$\text{IFR} = \sum_\alpha \frac{N_\alpha}{N} \text{IFR}_\alpha = \sum_\alpha \frac{N_\alpha}{N} h_\alpha c_\alpha d_\alpha \tag{8}$$

i.e., the infected person needs to make the transitions $I \to Q^c \to C \to D$. Note that we assume age-independent attack rates (infection probabilities) for the derivation of the population-wide IFR from the corresponding age-specific ratios IFR_α. The IFR as defined here also does not include extra deaths due to ICU overflow (see below). In the interactive application, we also refer to IFR as population-wide *mortality* due to SARS-CoV-2 (severe acute respiratory syndrome coronavirus 2, (WHO, 2020b)) infection.

If the value of the mortality (IFR) is changed in the interactive application, this is achieved in the model by rescaling h_α by the appropriate factor. We choose to rescale h_α, rather than c_α or d_α, because while c_α and d_α can be inferred with fairly high confidence from case statistics, h_α can only be inferred from random samples (Lavezzo et al., 2020; Mizumoto et al., 2020). In practice, estimates of h_α typically depend on the ability to detect infected cases (detection ratio δ).

ICU capacity and overflow ICU capacity is an important constraint during the course of the epidemic. The model therefore includes a number

- C_{ICU}: maximal number of ICU beds that are available to treat critical COVID-19 patients.

If the ICU capacity is exceeded, not all patients with ICU need can receive adequate care any more. This leads to an increased death rate for these patients, which is controlled by the parameter s.

- s: severity factor for ICU overflow. The probability that a critical patient dies is multiplied by s when required ICU care is not provided, $d_\alpha \to s\, d_\alpha$. If $s\, d_\alpha > 1$, we set $d_\alpha = 1$.

Excess death is incorporated into into the model as follows:

$$d'_\alpha = \frac{C_{\mathrm{ICU}}}{\sum_\alpha C_\alpha} d_\alpha + \Big(1 - \frac{C_{\mathrm{ICU}}}{\sum_\alpha C_\alpha}\Big) \min\{1, s\, d_\alpha\}, \tag{9}$$

where d_α and $\min\{1, s\, d_\alpha\}$ are the death rates of patients with ICU need, who do or do not have an ICU bed, respectively.

Optional 'locking' of IFR, detection ratio δ and initial cases I_0
If a user changes the number of infectious people in compartment I by some factor c, but changes the outflow fractions from I to the "detected" compartments H and Q by the inverse factor, i.e.,

$$I(t) \to c \cdot I(t)\,, \quad h_\alpha \to h_\alpha / c\,, \quad \delta \to \delta / c\,,$$

the model dynamics in all detected compartments (H, C, D, Q, $\mathrm{R^k}$) remain unaltered. Furthermore, a change in the *initial number* of infected people, $I(t_0) \to c \cdot I(t_0)$ leads *approximately* to a change of $I(t)$ by the same factor during the entire early phase of the epidemic (as long as most individuals are susceptible and assuming $E(t_0) = 0$; otherwise $E(t_0)$ also needs to be scaled). We therefore enable optional locking of these three parameters in the simulator to allow for changes in the IFR while maintaining the fit of the observed data.

3 Data

The intention of the SEIR model is to explore disease dynamics under various assumptions on the model parameters. In this sense, the web application offers the freedom to choose arbitrary values for almost all parameters. In order to target model scenarios to the COVID-19 outbreak in Austria, however, parameters should be linked to the available data. For some parameters, such as demography, precise information is available, for others, such as infection fatality ratios, only plausible parameter ranges can be estimated. Finally, several

parameters such as the mitigation strengths can only be estimated by fitting the SEIR dynamics to the documented case numbers. Below, we discuss our data sources and estimation procedures in detail.

3.1 Demographic data

For Austria, we use the age-specific population sizes (census 2019 of Statistik Austria - "Bevölkerung am 1.1.2019 nach Alter und Bundesland - Insgesamt"):

Age-class	Austria	Burgenland	Carinthia (Kärnten)	Lower AT (NÖ)	Upper AT (OÖ)
0-9	855,419	25,142	48,898	159,465	150,469
10-19	862,277	27,164	53,326	168,420	150,381
20-29	1,134,471	29,224	60,867	187,627	186,579
30-39	1,203,124	34,971	68,129	206,546	196,146
40-49	1,209,216	41,701	74,569	234,138	196,756
50-59	1,382,468	49,207	93,267	276,998	235,381
60-69	989,286	40,518	72,921	195,636	168,069
70-79	779,997	27,522	55,508	158,118	123,065
80+	442,517	17,984	33,454	90,594	75,249
Total	8,858,775	293,433	560,939	1,677,542	1,482,095

	Salzburg	Styria (Stmk.)	Tyrol (Tirol)	Vorarlberg	Vienna (Wien)
0-9	54,434	111,091	73,916	42,166	189,838
10-19	55,549	113,935	73,894	42,753	176,855
20-29	70,246	156,515	102,571	49,242	291,600
30-39	75,875	162,552	103,835	54,107	300,963
40-49	75,010	168,382	102,689	55,040	260,931
50-59	86,302	197,211	118,196	60,127	265,779
60-69	62,314	147,658	80,144	41,431	180,595
70-79	49,170	115,255	63,330	31,152	156,877
80+	26,321	70,453	36,130	18,279	74,053
Total	555,221	1,243,052	754,705	394,297	1,897,491

3.2 Epidemiological data

While some data to estimate the generation interval for the COVID-19 outbreak are available, estimates of the reproduction number rely on the observed dynamics of the epidemic in different countries.

Reproduction number

We use the following parameter ranges and estimation procedures for the parameters that influence the effective reproduction number $\mathcal{R}_{\text{eff}}$ (eq. 5a).

- For the basic reproduction number $\mathcal{R}_0$ of COVID-19, a wide range of estimates exists in the literature – depending on time, geographic location and estimation procedure. For the initial phase (January-February, 2020), estimates range from 1.4 to 6.5 (Liu et al., 2020; Park et al., 2020; Zhuang et al., 2020). Note that $\mathcal{R}_0$ depends on the interaction networks of a society and will therefore plausibly differ between countries and regions. For this reason, we estimate $\mathcal{R}_0$ from the Austrian case data, rather than fixing it to a predefined value derived for another location.

  In particular, we choose the value of $\mathcal{R}_0$ such that the daily increase in infections, Eq. (7), matches the reported daily increase in confirmed cases of about 30%, $\lambda \approx 1.3$. When using Eq. (7) for this purpose, we assume there was no mitigation/isolation active, take the value of seasonal reduction according to the scenario (below) from the 8th of March and use the values of t_l, t_i discussed below.

- Even more than $\mathcal{R}_0$, the mitigation strength $M(t)$ strongly depends on governmental actions and behavioural patterns that are highly country-specific (see international mobility data). In our scenarios, they are thus either estimated from the case data, or deliberately chosen to design hypothetical scenarios (e.g., *What would have happened without mitigation?*). There is more prior knowledge on plausible mitigation dates t_j, in particular the lockdown in Austria on March 16 that led to a marked reduction in mobility (see Austrian mobility data). Therefore, we make use of these dates in the scenarios.

- Seasonal amplitude: In our fitted scenario, we use $\epsilon = \{0, 0.1, 0.2\}$. The strength $\epsilon = 0.2$ for seasonality follows from the best estimate of Kissler et al. (2020). An upper estimate for the general seasonality of other coronaviruses in temperate climates (Monto et al., 2020) is $\epsilon = 0.5$. However, since COVID-19 has a higher effective reproduction number $\mathcal{R}_{\text{eff}}$, its seasonality may rather be weaker (Baker et al., 2020).

- Seasonal peak: We use t_{peak} on 15th January, following the estimate from Kissler et al. (2020).

- Isolation of age class α: In our current scenarios, we do not include any isolation of age classes (i.e., $\zeta_\alpha = 1$ for all α).

Generation interval

While the generation interval refers to the time between consecutive infection events, empirical data is usually rather available for the serial interval T_{SI}, which measures the time between the onset of symptoms of two consecutive (symptomatic) cases in a transmission chain. International estimates of $\bar{T}_{SI}$ range from about 4 (Du et al., 2020) to over 7 days (Lavezzo et al., 2020), with a large credible dataset supporting $\bar{T}_{SI} = 6$ (He et al., 2020). Through time, as testing and/or awareness increase, serial interval shortens (He et al.,

2020; Zhang, 2020). For Austria, AGES (Austrian Agency for Health and Food Safety) reports an expected value of 4.46 (Richter et al., 2020). The empirically estimated serial interval only accounts for recorded cases. Considering also unrecorded cases that do not quarantine, the generation interval is plausibly a bit longer. Based on our default estimates for T_l and T_i (see below), we obtain an expected generation interval of $\bar{T}_{GI} = T_l + T_i = 3 + 3 = 6$ days.

3.3 Disease outcome data

Outcome fractions

The transition probabilities between compartments (I: Infected, H: Hospitalised, C: Critical, D: Deceased) are based on estimates by Salje et al. (2020, for uniform attack rates across age classes). They also utilize data from the Diamond ship (Mizumoto et al., 2020) to remove the dependency of the I→H transition (h_α) on the detection ratio δ. We adjust the transition probabilities to be consistent with the Austrian case fatality ratio (CFR) per age-class and the overall infection fatality ratio (IFR) of 0.7%. The age-structured adjustment is also informed by Spanish and German data (MISAN, 2020; Schilling et al., 2020), and implicitly includes patients from care homes (excluded in Salje et al. 2020).

Age group	h_α	c_α	d_α
0-9	0.1	20	3
10-19	0.2	15	5
20-29	1	12	8
30-39	1.8	15	8
40-49	2.5	20	12
50-59	4	22	15
60-69	7.3	32	30
70-79	12	45	45
80+	30	50	50

Waiting times

The mean waiting times are ultimately fitted to our model to give the best fit (see below). The values are in a good agreement with existing literature.

- $T_l = 3$, *mean latency time*, i.e., time from getting infected but becoming infectious. The latency time must be shorter than the incubation period (time before symptoms appear), which is around 4 days (Böhmer et al., 2020; Guan et al., 2020) to 5 days (Lauer et al., 2020). See the discussion of the generation interval above for further references.
- $T_i = 3$, *mean time when infectious* consists both of the pre-symptomatic and symptomatic phase for symptomatic patients. We assume that the

pre-symptomatic phase on average about two days long (Hu et al., 2020; Zhang, 2020) and that the symptomatic phase when SARS-CoV-2 infected patients are still infecting the population is about one day. The infectious time is known to decrease during the course of the epidemic due to increasing awareness (Bi et al., 2020; Zhang, 2020; He et al., 2020). However, we neglect the longer infectious time in the early days of the epidemics, as the early data cannot be closely fitted due to under-reporting. Since there is no good data concerning the infectious time of asymptomatic carriers known to us, we assume the same values as for symptomatic patients. The asymptomatic proportion of about 50% (Lavezzo et al., 2020) therefore does not currently enter the model, although it does provide a bound to the I→H rate (h_α, above).

- $T_h = 11.5$, *mean time in hospital* summarizes the time in a normal hospital bed before recovery or transfer to an ICU. Literature estimates are around 12 days (Sanche et al., 2020; Zhou et al., 2020; Guan et al., 2020) or slightly shorter for COVID-19 patients who die (Zhou et al., 2020).

- $T_c = 6.5$, *mean time in critical care, ICU*. This time is fitted to ICU data and is in good agreement with Zhou et al. (2020), who report a mean time of around 7 days.

- $T_q = 10$: *mean time in quarantine* until a test for SARS-CoV-2 comes negative. We are not aware of existing estimates, but it appears reasonable to assume that it is slightly less than the time to recovery for the severe cases, $T_h = 11.5$.

COVID-19 detection and fatality ratios

Infection fatality ratio (IFR) Estimates of the IFR for COVID-19 from epidemiological models and serology studies vary widely. There are several reasons for this large variance and the high level of uncertainty.

- The true number of *COVID-19 deaths* (the numerator of the IFR) is uncertain and numbers from different countries often cannot easily be compared. In some countries (such as China and Iran), the official numbers of deaths cannot be trusted (Bessis, 2020), while in other countries only hospital deaths are counted and/or suspected COVID-19 deaths with a lacking PCR (polymerase chain reaction) test validation remain unrecorded. Further, estimates from excess mortality may also include deaths that are not (or not directly) related to COVID-19.

- The true number of *infections* (the denominator of the IFR) is even more difficult to obtain. Due to limited testing capacity and a large fraction of asymptomatic cases, the official number of recorded cases is usually much smaller than the number of true cases. Consequently, the ratio of known deaths to known cases, or *case fatality ratio* (CFR) overestimates the IFR.

The best estimates of true case numbers rely on serology studies in regions with high prevalence, although it should be noted that infections do not necessarily generate antibodies.

- The strong dependence of the IFR of COVID-19 on age and health status, as well as large differences in disease prevalence, make it very *difficult to compare IFRs among countries* and groups of people. For example, the Italian population is on average older than the Austrian one, while the population of New York City is younger. Within countries, samples need to be carefully designed to avoid spurious correlations.

In a Scientific Brief from August 4th, the WHO estimates worldwide IFRs between 0.5% and 1.0% (WHO, 2020a). Estimates for single countries and regions include the following [with 95% CI]:

- The largest serology survey to date, with more than 100 000 participants from across the UK, dating July 13, reports a country-wide immunity level of 6% (Ward et al., 2020). Based on these data, the REACT2 study team reports a country-wide IFR of 0.9% [0.86%; 0.94%] excluding care homes and an IFR as high as 1.58% [1.51%; 1.65%] if excess rather than COVID-specific deaths are used and care home deaths are included.

- An earlier large serology survey with more than 60 000 participants from across Spain, dating May 13, reports a country-wide immunity level of 5% (Centro National de Epidemiología, 2020). Based on these data, a study by the Spanish ENE-Covid group from August 7th (preprint) reports a country-wide IFR outside nursing homes of (95% CI) 0.83% [0.78%; 0.89%] if only confirmed deaths are included. Based on total excess mortality, this increases to 1.07% [1.00%; 1.15%] (Pastor-Barriuso et al., 2020).

- Two regional serology studies from Switzerland report IFRs of 0.64% [0.38%; 0.98%] for Geneva as of June 2nd (Perez-Saez et al., 2020) and 0.6% [0.4%; 0.8%] for the Canton of Zurich end of May (Emmenegger et al., 2020).

- An early small regional serological study from the heavily affected Heinsberg region in Germany reported an IFR of 0.36% [0.29%; 0.45%], based on 7 deaths at the time of assessment in the community of Gangelt (Streeck et al., 2020) (as of July 1st, the number of deaths has increased to 12).

- A modeling study combining French data with infection and fatality rates from the Diamond Princess cruise ship estimates an IFR of 0.53% (±0.2%) for France (Salje et al., 2020).

- Modeling results of the Imperial College COVID-19 Response Team on the state of the epidemic in the United States (May 21) estimate IFRs to vary across states between 0.7% and 1.1% (Unwin et al., 2020). Differences are mainly due to variation in age structure.

- Based on an SEIR model, Hauser et al. (2020) report IFRs for Hubei, China 2.9% [2.4%; 3.5%] and 6 European regions, ranging between 0.5% and 1.4%.
- Another model based on CFRs, corrected for testing capacities, estimates worldwide IFRs in 139 countries with an average of 1.04% (ranging from 0.77% to 1.38%) (Grewelle and De Leo, 2020).
- A recent meta-analysis of 25 studies from PubMed and MedRxiv on the IFR until May 21st reports an average IFR of 0.64% (in $[0.50\%; 0.78\%]$) (Meyerowitz-Katz and Merone, 2020).
- On August 20st, the gross death rate in New York City due to COVID-19 derives to $23\,639/8\,400\,000 = 0.28\%$ (including probable COVID-19 deaths, but not including excess mortality) (New York Health Dep., 2020). The gross death rate is highest for The Bronx, at 0.35%. These values represent strict lower bounds for the regional IFR. Antibody tests point to immunity levels of $25 - 40\%$ in NYC (Kim, 2020), consistent with an IFR of around 1%. An estimate of 0.85%, based on data from April 22 may be found in another preprint (Wilson, 2020).

Austria

- The only published estimate of an IFR for Austria (to our knowledge) is based on an SEIR model and relies on data from the early outbreak in March and April. Hauser et al. (Hauser et al., 2020) report 1.1% (95% CI 0.8, 1.3) using data up to April 11th.
- As of August 20, Austria has reported 24 236 confirmed SARS-CoV-2 infections and 724 COVID-19 deaths according to the *Gesundheitsministerium* (Austrian Health Ministry, 2020), corresponding to a formal CFR of 3%. Of the confirmed cases, 2609 cases are still active, which may lead to a undercount of deaths. More importantly, the reported cases represent only a fraction of the true cases. This fraction is unknown and there are only rough estimates.
- In early April, a SORA PCR random study estimated 28 500 (95% confidence interval $[10\,200, 67\,400]$) infected and PCR detectable individuals in Austria (excluding hospitals) (Ogris et al., 2020). This number should be compared with $\sim 8\,000$ known active cases outside of the hospitals at the same time. This evaluates to a formal *detection ratio* δ of 28%, with a large confidence interval $[12\%; 78\%]$. Imperfect sensitivity of the test (leading to false negatives) and reporting delays for the number of recovered people lead to an upward bias of these numbers, while low specificity (false positives) leads to a downward bias. For a maximal plausible deviation due to testing errors, SORA assumes 50% sensitivity and perfect specificity, leading to an additional factor of 2 in the estimated disease prevalence and $\frac{1}{2}$ for the detection ratio.

- A second PCR study by Statistik Austria up to April 24 resulted in an *upper limit* (95% CI) of 10 823 infected individuals (older than 16 and excluding hospitals), which should be compared with $\sim$ 2 200 known active cases outside of the hospital older than 16 at the same time. No point estimate was reported, but the result is broadly consistent with the SORA study (with 20% as lower limit for the detection ratio in April).

- Imperial College COVID-19 Response Team et al. (2020) estimate that on May 4th, 0.76% of the Austrian population ($\sim$ 67300 people) had been infected. With 15630 detected cases on the same date this evaluates to an average δ of 23.2% by this date.

- The detection ratio $\delta(t)$ during the epidemic is not a constant, but increases with increasing awareness, increased PCR testing capacities (in particular in March and April) and increasing contact tracing to detect also asymptomatic cases (in particular in the later phases in May and June). Indeed, an antibody study in the heavily affected Tyrolian community of Ischgl (data collected between April 21st and 27th) with many infections as early as February resulted in an immunity level of 42% and a ratio detection ratio of 15% at the lower end of the confidence interval derived above. Increased testing led to a sharp decline in the proportion of positive PCR tests in April, from $> 15\%$ to $< 1\%$ (Roser et al., 2020). Subsequently, testing and tracking of infection clusters was improved. It appears plausible that by July/August most symptomatic cases and a share of asymptomatic cases are being detected.

Weighting all the evidence, we arrive at a plausible value around 0.7% for the IFR in Austria. With this value, the fit to the case and death data implies a detection ratio δ of 15% for the initial phase of the epidemic (until the end of March), in accordance to the observations from Ischgl. After this phase, we assume that the detection probability gradually (in the model: linearly) increases and reaches 47% by May 18th.

While these are the default values used in our scenarios, we stress that they come with a large uncertainty. A "true" IFR between 0.3% and 1.1% (with corresponding initial δ between 6.4% and 23.6% until end of March) appears to be possible. It is left to the user to adjust these values.

ICU overflow and excess death rate An unmitigated, fast-spreading epidemic in a population without prior immunity readily leads to more than 10% of the total population being *simultaneously* infected and imposes extreme strain on any health care system. For COVID-19, this holds, in particular, for the ICU wards, because many patients with severe symptoms require long-term intensive care. In the past months, the health system in several regions (New York, Madrid, London, Alsace) has been pushed to its limits. In two regions (Wuhan and Bergamo) it has been temporally overwhelmed. The gross death rate related to SARS-CoV-2 in the Bergamo province has been estimated from

excess mortality (until May 9) as 0.58% (Modi et al., 2020). For all of Italy, Grewelle and De Leo (2020) estimate an IFR of 1.91% (reflecting a high CFR despite high testing rates). Preliminary data from a large-scale serology study point to country-wide antibody levels of only 2.5% (ISTAT, 2020), consistent with a high IFR $\gg 1\%$.

Based on Gesundheitsministerium data, we assume that the maximal ICU capacity for COVID-19 patients is around $ICU_{\text{capacity}} = 1000$. However, the number of total ICU beds has been decreasing over the course of epidemic from about 1200 ICU beds (early) to < 800 beds (end of June).

We assume that the severity factor is around $s = 2$, i.e., the death rate doubles for critically ill patients who require intensive care, but cannot receive it because the ICU capacity is exceeded. This seems plausible, considering the high estimates of the Italian IFR.

3.4 Case data

We use data from two official webpages of the Austrian Ministry for Social Affairs, which we refer to as:

- Sozialministerium (SM) website and
- Gesundheitsministerium (GM) website.

The scraping of the two websites is done by running 'Scraping_ministry_new.ipynb', which can be found in the data folder of the GitHub repository, together with all the files mentioned below.

SM website

This scrapes complete Bundesland-specific data from this website, which:

1. are stored daily as presented in the webpage (in folder 'sozialministerium_daily').
2. are used to update the files 'confirmed.csv', 'deaths.csv', 'recovered.csv', 'all_hospitalized.csv', 'icu_hospitalized.csv', 'tested.csv'.
3. are used to update the 'whole_country_data.csv' (used for whole-country fitting, see below for more details).
4. are used to update Bundesland-specific data ('BundeslandName.csv') for all categories above (used for Bundesland-specific fitting).

Some notes on SM data:

- These are **not back-updated data**. This means that once a day has passed, its data remains constant. Back updating would be typically applied in cases such as a sample that was taken on day x but its positive diagnosis is submitted to the authorities on a later day $x + y$. This would give a sampling date-based data set, e.g., where incidences at current time are underestimated. Then the positive cases from day x would have to be incremented based on information received on day $x + y$ (back-update).
- If the code is run more than once daily the content is **not** modified, since the webpage is only updated once a day (at 09:30, except for 'confirmed', which is updated at 08:00 and 15:00, but we try to consistently get data from 08:00).
- Bundesland-specific data for 'tested' were not available until 15.04, so data in 'tested.csv' are available from 2020-04-15.
- Some Bundesländer do not update the data on some days, which is indicated with a '+' on that particular date. For example, '172+' means that on the previous day there were 172 cases and that the data for that day will be incorporated into the following's (e.g., data for Vienna on 01-06-2020).

GM website

This scrapes data from CSV files provided on the dashboard, which:

1. are stored daily as extracted (in folder 'gesundheitsministerium_daily/[date]').
2. are used to update the **back-updated data** for 'confirmed', 'deaths' and 'recovered' (using 'Epikurve.csv', 'TodesfaelleTimeline.csv' and 'GenesenTimeline.csv') in 'whole_country_data.csv' (used for whole-country fitting, see below for more details)
3. are used to append the daily back-updated 'confirmed', 'deaths' and 'recovered' (corresponding to columns d, e, f of 'whole_country_data.csv' - see below) to 'reporting_delay_confirmed.csv', 'reporting_delay_deaths.csv' and 'reporting_delay_recovered.csv', respectively. These data are used to estimate the delay in reporting of all three categories.
4. are used to update other files: 'ageDistrib_confirmed.csv', 'ageDistrib_deaths.csv', 'ageDistrib_deathsPer100000.csv', 'districts.csv', 'sexProportion_confirmed', 'sexProportion_deaths'. For each is '[nameOri]: explanation', where nameOri.csv is the name of the file as downloaded from the GM website with the 'CSV download' option):
    - ageDistrib_confirmed.csv (Altersverteilung): distribution of ages of confirmed cases

- ageDistrib_deaths.csv (AltersverteilungTodesfaelle): distribution of ages of deaths
- ageDistrib_deathsPer100000.csv (AltersverteilungTodesfaelleDemogr): distribution of ages of deaths (per 100 000 inhabitants)
- districts.csv (Bezirke): confirmed per district (in absolute numbers)
- sexProportion_confirmed.csv (Geschlechtsverteilung): proportion of sexes of confirmed
- sexProportion_deaths.csv (VerstorbenGeschlechtsverteilung): proportion of sexes of deaths

Notes on GM data:

- If the code is run more than once daily the content is updated.

On 'whole_country_data.csv'

Data used for whole-country fitting. Description of the columns in "whole_country_data.csv" file:

1. Data from SM (not back-updated) in: 'confirmed_nobackupd', 'deaths_nobackupd', 'recovered_nobackupd', 'all_hospitalized' (a), 'icu_hospitalized' (b), 'tested' (c)
2. Data from GM (back-updated): 'confirmed' (d), 'deaths' (e), 'recovered' (f)

For whole-country fitting, we use a, b, c (not back-updated) and d, e, f (back-updated).

Note that even the back-updated data suffer from a reporting delay. First, the daily reports summarise the events of the *previous* day. Second, the cases are dated to when a positive test result was obtained, not to when the test was administered, or when the patient was identified and quarantined. We account for this delay in the model by shifting its output appropriately – see Sec. 3.5.

3.5 Solving and fitting the model

The ODE system in equations (1) is numerically solved using the default initial value problem solver (RK45) of the *Python SciPy* library (Virtanen et al., 2020) via the `scipy.integrate.solve_ivp` function. Two procedures have been implemented. First, an explicit solution of the full model with age-specific ODEs. Second, in the special case of a temporally stable age distribution in all nonterminal compartments, we speed up the computation by solving the ODEs after summing over the age classes. Age distributions in each compartment can be derived from the stable distribution in a separate step. This is possible because

our model assumes age-independent attack rates and initial distribution of infected individuals, which corresponds to the overall age distribution. To get the cumulative number of *confirmed cases* from the data and the model dynamics, we take the sum $R^k + Q + Q^h + Q^c + H + C + D$.

Accounting for reporting delay. Before fitting the model to the data, or displaying it in the interactive application along with the data, we account for the reporting delay in the data. This is done by shifting selected compartments in the model output forward in time by a suitable number of days. Specifically, the Q^*, H, C and R^k compartments, as well as the cumulative *confirmed cases*, are shifted forward by 2 days. This is because new cases are typically reported with the day of a positive test result, and therefore at least two days after the patient is identified and isolated (and therefore leaves the I compartment). The D compartment (which is back-updated) and all the remaining compartments (i.e. the individuals who have not been infected, or have not been detected) are not shifted.

The parameter fit is a heuristic process, not fully automatized. Most parameters are informed primarily by the literature, as described above. The following automatic method was implemented to aid this heuristic approach. We minimise the cost function

$$F = \sum_{\alpha,t} w_\alpha \frac{(y^*_{\alpha,t} - y_{\alpha,t})^2}{(y^*_{\alpha,t} + y_{\alpha,t})}, \tag{10}$$

where $y^*_{\alpha,t}$ is the data point on day t for the compartment

$$\alpha \in \{\text{Confirmed cases, Hospitalized, Critical, Deceased}\} \tag{11}$$

and $y_{\alpha,t}$ is the corresponding model prediction. Recovered cases are not used for the fit as we consider that even the detected (known) recovered cases are underreported in the data, especially in the early days. Dividing the squared difference by the mean value is loosely inspired by Poisson noise. The weight w_α is chosen to be $w_\alpha = 0.1$ for Hospitalized patients, $w_\alpha = 0.3$ for Confirmed cases and $w_\alpha = 1$ otherwise. This reflects the fact that confirmed cases and hospitalizations are the most numerous, but not necessarily the most reliable. After this correction, the time-series of (more numerous) confirmed cases has a similar weight to the time-series of the deceased, while counts of hospitalised patients are assumed to be less reliable. In addition, we discard data points with low case count (Threshold 100 for confirmed cases and 10 for H, C, D compartments). The cost function F is minimized using the Nelder-Mead method implemented in *Python SciPy*'s minimize function. Due to high dimensionality of the problem, we minimize F with respect to subsets of parameters at a time (see also scenario 1 below).

4 Application

On this page, we apply the simulation model to several basic scenarios for the spread of the disease and briefly discuss what we can (and cannot) learn from these scenarios for the actual outbreak in Austria.

4.1 Scenario 1: Best fit for Austria

A canonical use of the simulator is to try and fit the model to the Austrian case data for people with a detected infection, patients in hospital and ICU wards, and the recorded COVID-19 deaths. We provide three such "best fit" scenarios with our simulator, for different assumptions on the effect of seasonality on the spread of the virus. Below, we briefly discuss the main steps of the fitting procedure and the results of the simulations.

Fitting of $\mathcal{R}_{\mathbf{eff}}(t)$ and other parameters

In a first step, we match the initial $\mathcal{R}_0$ to the $\sim 30\%$ daily increase ($\lambda \approx 1.3$) in case data that was observed in Austria prior to the lockdown. Assuming an IFR of 0.7% and using estimates for transition rates and waiting times from the literature (see above), we then focus on the fit of the initial number of infected cases I_0 and a single mitigation step at some time t_1. Consistent with the Austrian lockdown, our estimate of t_1 indicates a change in $\mathcal{R}_{\text{eff}}$ around March 16^{th} ($\pm$ 1 day). We also adjust the waiting times for the best fit, keeping the generation interval to $T_{\text{SI}} = 6$ ($T_l = 3$, $T_i = 3$). At first, we assume a step change in the detection ratio δ, increasing at some point in late spring.

Next, we include a total of four switch-dates for changes in mitigation. We fix the first mitigation date t_1 on March 16^{th}, as already mentioned above. The second and third switch dates t_2 and t_3 parameterize the relaxation of the lockdown starting on May 1st (opening of shops, gradual relaxation of gathering and travel). The second and third switch-point are only two weeks apart and reflect fast increase in the virus transmission as the rules were relaxed: the third switch point t_3 is fitted to May 15^{th}. The fourth switch-point t_4 is fitted to July 22^{nd}, and accounts for slightly reinforced measures (such as mask wearing and renewed travel restrictions).

Finally, we fit all four mitigation strengths together with the time-dependent detection ratio $\delta(t)$. The estimated detection ratio is 15% before April 1^{st}, linearly increasing to 47% from May 18^{th}. This is consistent with the changing numbers of of COVID-19 tests and the positivity ratio. We re-adjust the waiting times in the various compartments, notably the times at hospital and at the critical care – and the quarantine times before admission.

Seasonality

We explore three basic amplitudes: no effect ($\epsilon = 0$), weak ($\epsilon = 0.1$) and moderate seasonality ($\epsilon = 0.2$). The rationale for these values is explained in Section 3.2 above.

Without seasonality ($\epsilon = 0$), the fitting procedure described above leads to values of the basic reproduction number $\mathcal{R}_0$ between 3.2 and 3.33 (depending on seasonality) and reproduces the approx. 30% daily increase in case data that was observed in Austria prior to the lockdown. As described above, we include four switch-dates for changes in mitigation. Given these dates, we estimate values for $\mathcal{R}_0$ and for mitigated values $\mathcal{R}_i$ as shown in Table 1.

Table 1: The table shows the basic reproduction number $\mathcal{R}_0$ and the mitigated reproduction numbers $\mathcal{R}_i = \mathcal{R}_0(1 - M_i)$ after the i^{th} switch point. Rows correspond to different strength of the seasonal effect.

ϵ	$\mathcal{R}_0$	$\mathcal{R}_1$	$\mathcal{R}_2$	$\mathcal{R}_3$	$\mathcal{R}_4$
0	3.2	0.58	0.67	1.14	1.03
0.1	3.26	0.60	0.73	1.25	1.16
0.2	3.33	0.62	0.82	1.39	1.32

With seasonality, the basic reproduction number $\mathcal{R}_0$ for the best fit increases. This is because seasonality reduces the effective reproduction number $\mathcal{R}_{\text{eff}}(t)$. Hence, for any observed growth of the infections, the underlying $\mathcal{R}_0$ must increase to compensate this effect. We derive $\mathcal{R}_0$-values for all seasonal scenarios such that the initial daily increase in the cumulative number of infected cases stays at 30%.

We then fit all mitigations jointly for the different seasonality strengths (ϵ) using the best fit in the absence of seasonality for all other parameters. The results for the mitigated reproduction numbers $\mathcal{R}_i$ are summarized in Table (1). Note that these values only reflect the effects of governmental interventions and behavioral changes in response to the virus, but not the effects of seasonality and of emerging immunity from recovered individuals.

For all levels of seasonality, the initial number of infectious cases is estimated to $I_0 = 490$ on March 1st, 2020. Detection ratio increases from an early estimated value of $\delta = 15\%$ to current 47%.

In our scenarios, we have assumed four switch-points for the effect of mitigation measures and adjusted the date and strength of these changes to the case data accordingly. Note that this does not mean that the reproduction number has changed only at these points in time (see also our R-Nowcasting page). However, if more switch-points are assumed, the signal from the available data is still too weak for an accurate parameter estimate. We invite the user to explore the effects of further switch-points.

Infection fatality ratio (IFR) and detection ratio

In contrast to the reproduction number parameters, the mortality of COVID-19 cannot be estimated from the case data. The reason is that the IFR = deaths / cases, has the true number of infections in the denominator, which however depends on the probability that these cases are detected and included into the official records. This detection ratio ($\delta(t)$) is not well known and can only be roughly estimated. From two Austrian PCR surveys (SORA and Statistik Austria), an antibody study at Ischgl and a range of international studies, we arrive at plausible values of 0.7% for the IFR and 15% for the detection ratio during the early phase of the epidemic (until April 1^{st}). With increased testing and contact tracing, a much higher proportion of infections was detected at later stages of the outbreak, as evidenced by a sharp decline in the percentage of positive PCR tests. This is included into the model as a linear increase of the detection ratio until May 18^{th}, where it reaches 47% in the best-fit scenario. However, these values come with a large uncertainty and a "true" IFR between 0.3% and 1.1% (initial δ between 6.4% and 23.6%) appears to be possible. See the documentation and the Scope & Limits section for further arguments and references.

Results: Outbreak dynamics

The outbreak dynamics with different levels of seasonality ϵ are shown in the following figures.

The bottom panels of Figures 1, 2, 3 show how the effective reproduction number $\mathcal{R}_{\text{eff}}(t)$ changes over the same time scale for the seasonal scenarios. In particular, we see which factor contributes most strongly to the reduction of the maximal level of transmission (corresponding to the fitted $\mathcal{R}_0$).

We see that the estimated level of current mitigation ($\mathcal{R}_4$) is sufficient to keep the virus largely under control in the absence of seasonality ($\epsilon = 0$, Figure 1). Although new infections continue to occur, there is no stress on the health system and the total number of COVID-19 deaths in Austria remains moderate. The population-wide level of "herd" immunity due to people who have recovered from the disease remains very low throughout.

A contrasting outcome is obtained under the assumption of moderate seasonality ($\epsilon = 0.2$, Figure 3). In this case, the current low level of transmission is partially due to the seasonal effect rather than due to behavioral changes. Assuming that the behavioral pattern remains constant, the total mitigation proves insufficient in winter and a second wave of infections is triggered. Since our model does not include a (likely) response to this wave in terms of reinforced mitigation measures, we see a steep increase in the number of infections and deaths until the further spread is eventually stopped by a combination of emerging immunity, seasonal effects and behavioral mitigation.

Finally, the case of weak seasonality ($\epsilon = 0.1$, Figure 2) produces a "weak second wave" that does not overwhelm the health system, but still leads to

Figure 1: No seasonal effects, $\epsilon = 0$

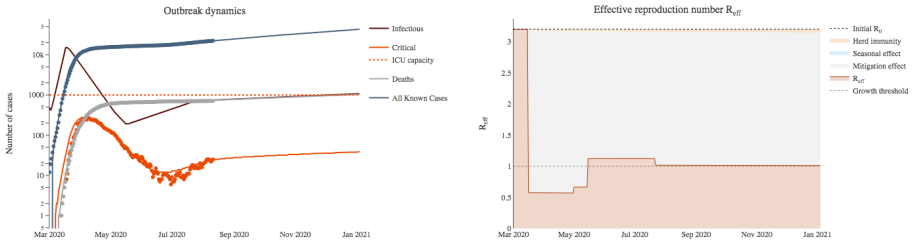

Figure 2: Weak seasonality, $\epsilon = 0.1$

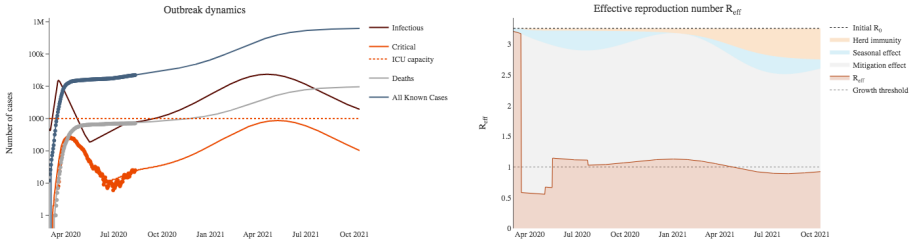

Figure 3: Moderate seasonality, $\epsilon = 0.2$

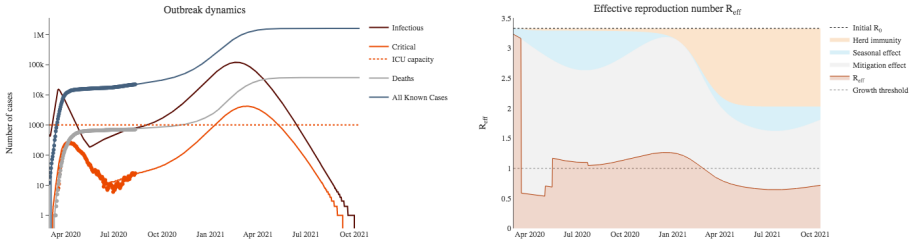

more than a million of infections by summer 2021 in the absence of changes in behavior – or a vaccination.

4.2 Scenario 2: Epidemic spread without (or with insufficient) mitigation

The use of the SEIR model is not limited to the attempt to provide best fits to actual case data. It can be equally instructive to explore hypothetical scenarios. A natural reference scenario in this sense addresses the question: What would happen without any mitigation due to either governmental interventions

or spontaneous behavioral changes by the population in response to the disease? Or, to rephrase the question: What would happen if we deal with COVID-19 in the same way as we deal with a normal flu season – only without the possibility of vaccination and without acquired (partial) immunity?

To address this question, we maintain all parameters of the "best fit" model described in Scenario 1 (including the initial conditions), but discard all mitigation steps. For simplicity, we focus on the case of no seasonality. In this case, the epidemic continues to grow with its initial rate (corresponding to $\mathcal{R}_0 = 3.2$) until it is stopped by emerging herd immunity. As in *Scenario 1*, we assume a default infection fatality ratio (IFR) of 0.7%. The resulting outbreak dynamic is displayed in the Figure 4.

Figure 4: Epidemic dynamics without mitigation

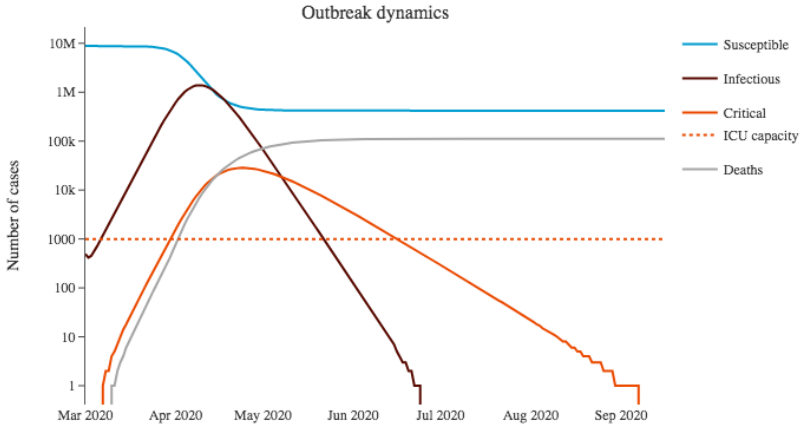

We see that the disease quickly overwhelms the health system and especially the ICU capacities. At the peak of ICU need, more than 28 000 patients simultaneously require intensive care, while only around 1 000 ICU beds are available in Austria.

As a consequence, a large majority of critical cases are not able to receive intensive care. Note that this effect is rather robust with respect to the number of available ICU beds. If instead of 1 000 there were 2 500 ICU beds available for COVID-19 patients (a theoretical upper bound when all Austrian capacities would be used for this purpose), the percentage of patients who can obtain adequate intensive care still remains low.

Our model assumes that this catastrophic overflow increases the death rate for all patients who cannot receive adequate care. Our scenario calculations use

an "ICU overflow severity factor" of 2 (corresponding to an increased average IFR of 1.4% for these patients). This way, we obtain more than 112 000 COVID-19 deaths by the end of the epidemic.

As a variation of the above "no mitigation" scenario, we can further ask what happens if governmental interventions and spontaneous behavioral changes do lead to a limited reduction of virus transmission, measured as the mitigated reproduction number $\mathcal{R}_1 = \mathcal{R}_0(1 - M_1)$, where M_1 is the mitigation strength that was achieved. Figure 5 explores this (in terms of the total number of expected deaths) for an assumed mitigation start date on March 16^{th} for three different baseline IFRs, at 0.3%, 0.7%, and 1%. We assume a severity factor of 2 for ICU overflow in all cases.

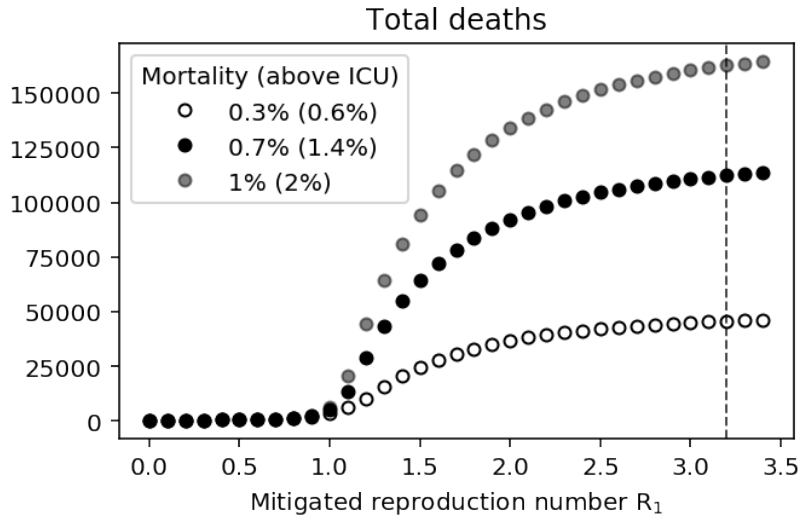

Figure 5: Total number of deaths over $\mathcal{R}_1$, for different IFRs in the unmitigated scenario.

As expected, the results show a linear dependence of the total number of deaths on the assumed IFR. In contrast, the dependence on $\mathcal{R}_1$ is highly non-linear with a threshold behavior at $\mathcal{R}_1 = 1$. Once $\mathcal{R}_1$ is clearly and consistently larger than 1, the death toll of the disease is unavoidably catastrophic.

For $R_1 = 1.3$ or larger, the death toll is in the order of tens of thousands, even if the infection fatality ratio IFR is as low as 0.3%. The reason is that in all these cases a large part of the Austrian population would get infected within a short period. Herd immunity will eventually stop the pandemic, but this will only happen after a period of extreme stress on the health system.

As an example, consider $\mathcal{R}_1 = 1.7$. In this case, more than 2/3 of the population (more than 6 million Austrians) get infected within half a year.

Note that this number is larger than the nominal herd immunity level $1 - 1/\mathcal{R}_1$ (about 41% for $\mathcal{R}_1 = 1.7$) that stops the spread of a new epidemic. An ongoing epidemic stops later since new infections still happen while the total number of infections declines (so-called *infection overshoot*). This again necessarily leads to severe ICU overflow, where a large majority of cases will not be able to receive intensive care. The death toll therefore reaches almost a level of twice the baseline IFR times 6 million (36 000 to 120 000 deaths in the IFR range considered).

A recent article in Nature by Flaxman et al. (2020) estimated that the lockdown in Austria saved between 40 000 and 85 000 lives by early May. These numbers are entirely in line with our hypothetical "no mitigation" model. Importantly, these model estimates are not meant to predict the real course of the disease, but depend on the assumption of a constant mitigation level. Accumulating deaths and a stressed health system almost necessarily lead to governmental interventions and spontaneous behavioral changes by the population, as seen in many countries with large initial case numbers.

Instead, the scenario refutes claims that COVID-19 is comparable to seasonal flu and shows that significant mitigation measures, driving $\mathcal{R}_1$ below 1, are unavoidable.

It also reveals that a strategy of insufficient mitigation, based on a hope that herd immunity will bring the pandemic to a halt, leads to a catastrophic death toll. This is expanded in more detail in *Scenario 3*.

4.3 Scenario 3: Herd immunity strategy

Herd immunity has been considered by some as a potential exit strategy from the epidemic. To achieve herd immunity, a substantial fraction of the population must gain immunity – which, in the absence of immunisation by a vaccine, requires contracting and overcoming the disease. To avoid serious healthcare overload which would increase mortality, this large number of infections must be spread out over a sufficiently long period of time. A natural question to ask is: What is the shortest time in which it might be feasible to achieve herd immunity, without overloading the healthcare system?

In Fig. 6, we show a scenario where the mitigation measures are as limited as possible – to allow the development of herd immunity, while still preventing ICU overload. In practice, implementing such measures would be difficult due to stochasticity and uncertainty about the outbreak at any given time. For this reason we require that in our deterministic model, the number of critical COVID-19 patients at any given time is at most 750 – less than the total ICU capacity of 1 000. Given the fraction of infected individuals who require critical care, and the assumed average of $T_c = 6.5$ days in ICU, this constraint translates to at most 6 600 new infections per day. All other parameters are assumed to be the same as in the "best fit" scenario above, with no seasonal effects.

As shown in Fig. 6, herd immunity would under these constraints be achieved

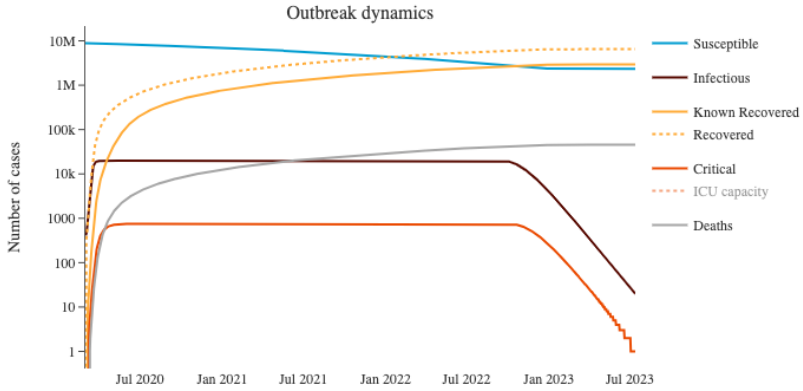

Figure 6: Outbreak dynamics in Austria in a scenario where herd immunity is achieved without overloading the intensive care unit.

in late 2022 – early 2023. By the time that the epidemic subsides, about 6.5 million people have overcome the disease (73% of the population), while about 2.3 million remain susceptible. Given the IFR of 0.7%, around 45 700 people would die of COVID-19. Throughout the process, especially in the early stages when most of the population is still susceptible, strong mitigation measures are necessary to prevent the epidemic from further growth. Early on, mitigation as strong as $M = 68\%$ is necessary, but this can be gradually relaxed, with complete lifting possible in late 2022.

The healthcare load, as well as the number of deaths, could be reduced if the most vulnerable groups were specifically isolated. This is not included in the scenario.

4.4 Scenario 4: Impact of lock-down timing (sensitivity analysis)

Upon pressing the "Recompute" button, the SEIR simulator derives a model output (curves for number of cases in each category, total number of deaths, etc.) from a set of input parameters, including the reproduction number R_0, mitigation strengths and times, and the transition probabilities and times between the model compartments. This points to another key usage of the SEIR simulation app – beyond fitting and the construction of purely hypothetical scenarios: providing a tool for the user to explore how (small) changes in the input parameters change the output.

In mathematical modeling, an analysis of this kind is called "local sensitivity

analysis". It is used (among other things) to assess the relative importance of certain input parameters for the model output. As an example, we will consider here two output quantities: the peak ICU need and the total number of COVID-19 deaths by August 31^{st}, 2020. We study how these quantities depend on two key input parameters, the timing of the lockdown (the first mitigation switch-point) and the timing of the relaxation of lockdown measures (starting with the second mitigation switch-point) that we have used in our "best fit" scenarios. All other parameters are kept constant, including, in particular, the strength of the mitigations.

Figure 7 shows the impact of a shift in the lockdown date (t_1) and all following switch-dates (t_2 - t_4) by a given number of days on the total number of deaths and the peak ICU need for three seasonal scenarios, with no, weak and moderate seasonal effects ($\epsilon = 0; 0.1; 0.2$). For all three scenarios, we obtain large changes for earlier or later lockdown dates, relative to our estimates with lockdown on March 16^{th} , see also Table 2.

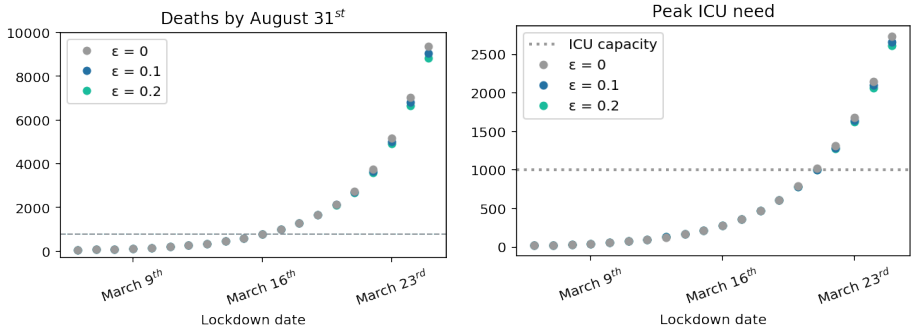

Figure 7: Impact of a change in the lockdown date on the total number of deaths and the peak ICU need for three seasonal scenarios, with no, weak, and moderate seasonal effects.

Table 2: Effect of the lockdown date (no / weak / moderate seasonal effects)

Lockdown date	**Deaths by August 31st**	**Peak ICU need**
March 16th	773/775/776	280/281/282
March 23rd	4 958/4 808/4 691	1 683/1 648/1 629
March 9th	128/132/135	44/45/45

Delay of the lockdown by one week leads to $\sim$ 6 times larger number of deaths and an overflow of the ICU capacities for all scenarios. Vice-versa, there is also an effect of an earlier lockdown, leading to $\sim$ 6 times lower total death numbers for a shift of one week. Note that the total lockdown period (time from lockdown to relaxation) is not changed in these scenarios.

In Figure 8, we analyze the impact of an earlier or later switch-point to relax the lockdown measures again (where we shift all switch-dates t_2 – t_4 after the lockdown by a set number of days), see also Table 3. In contrast to the previous case, we thus have a change in the lockdown period.

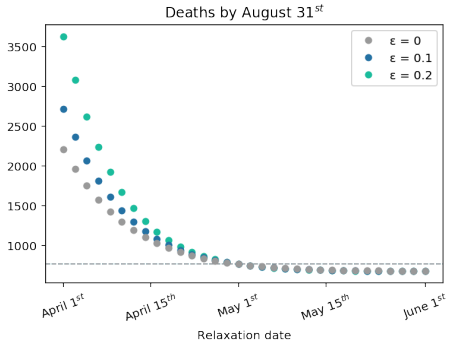

Figure 8: Impact of an earlier or later switch-point to relax the lockdown measures again.

Table 3: Effect of the date when mitigation measures are relaxed again (no / weak / moderate seasonal effects)

Relaxation date	**Deaths by August 31st**
May 1st	773/775/776
April 1st	2 265/2 802/3 693
June 1 st	683/682/681

The sensitivity of the total number of deaths to a shift in the relaxation date is smaller than for a shift in the lockdown date. This is expected because the absolute change in mitigation at this switch-point is smaller, but note that we also display much larger shifts by up to one month. While an earlier relaxation date on April 1^{st} can lead to a 4-fold increase of total deaths, the effect of a shift of the relaxation switch-point to an even later date is very small.

It is tempting to interpret these findings as predictions for what would have happened if the Austrian government had chosen an earlier or later lockdown date (or relaxation date). Such an interpretation has been made for related studies. However, we want to remind the user that this amounts to an over-interpretation. Neither our model, nor any other model known to us, can predict the behavioral changes of the Austrian population for scenarios that did not happen. Our derivations assume that no behavioral change would have happened other than the assumed temporal shift.

What can be concluded is the fact that the course of the epidemic is highly sensitive to the date of a lockdown of the estimated strength, and to a lesser degree to the relaxation date. It is very likely that both a (relatively) early lockdown and not-too-early relaxation contributed to Austria's successful course through the epidemic so far, but our sensitivity results should not be read as predictions for the number of saved lives (or extra deaths) for alternative governmental actions.

Further remarks:

1. Our results on the effect of a shift of the lockdown date on the peak ICU need shows good qualitative agreement with the results from the individual based simulation model by N. Popper (Bicher et al., 2020). This demonstrates the robustness of our (and Popper's) analysis with respect to modeling details.

2. In our sensitivity analysis above, we have only changed a single input parameter type (mitigation switch-points). For a complex problem with many interacting parameters (as we have it here), this simple view is often not sufficient. As an example, consider the three parameters "infection fatality ratio (IFR)", "detection ratio" and "initial number of infectious individuals". If any one or two of these parameters are changed, we observe strong effects on the model output. However, if we change all three in a coordinated way, there are almost no effects for the early phase of the epidemic, where data already exists. This is the reason why we have added the "lock" function to the input panel.

3. Sensitivity analysis is often also used to quantify the uncertainty of model predictions. If input parameters are known with some uncertainty that can be quantified, sensitivities translate these into uncertainties of the output. Some COVID-19 simulators (e.g., by Basel University: COVID-19 simulation tool) include this functionality and display credible intervals for the output. However, an interpretation of these credible intervals is not straightforward. This is because it is often not clear, which parameters are "known" with which uncertainty. In applications, we often use a best fit to output data (time series of past cases and deaths) to obtain estimates for input parameters, which then produce further estimates of output data (future cases). In addition, the parameter space of the model is large, making a comprehensive statistical analysis prohibitive. For this reason, we encourage the user to build her or his own intuition of model uncertainties by running the simulator in parameter regions of interest. Note that we do provide credible intervals for our R-Nowcasting, which is a much simpler problem. However, even in this case, the interpretation of the uncertainties displayed requires great caution (see our discussion there).

5 Sources

References

Austrian Health Ministry (2020). Amtliches Dashboard COVID19. https://info.gesundheitsministerium.at (2020-05-28).

Baker, R. E., Yang, W., Vecchi, G. A., Metcalf, C. J. E., and Grenfell, B. T. (2020). Susceptible supply limits the role of climate in the early sars-cov-2 pandemic. *Science*.

Bessis, D. (2020). Coronavirus: the key numbers we must find out. Library Catalog: medium.com.

Bi, Q., Wu, Y., Mei, S., Ye, C., Zou, X., Zhang, Z., Liu, X., Wei, L., Truelove, S. A., Zhang, T., Gao, W., Cheng, C., Tang, X., Wu, X., Wu, Y., Sun, B., Huang, S., Sun, Y., Zhang, J., Ma, T., Lessler, J., and Feng, T. (2020). Epidemiology and transmission of covid-19 in shenzhen china: Analysis of 391 cases and 1,286 of their close contacts. *medRxiv*.

Bicher, M. R., Rippinger, C., Urach, C., Brunmeir, D., Siebert, U., and Popper, N. (2020). Agent-based simulation for evaluation of contact-tracing policies against the spread of sars-cov-2. *medRxiv*.

Böhmer, M. M., Buchholz, U., Corman, V. M., Hoch, M., Katz, K., Marosevic, D. V., Böhm, S., Woudenberg, T., Ackermann, N., Konrad, R., Eberle, U., Treis, B., Dangel, A., Bengs, K., Fingerle, V., Berger, A., Hörmansdorfer, S., Ippisch, S., Wicklein, B., Grahl, A., Pörtner, K., Muller, N., Zeitlmann, N., Boender, T. S., Cai, W., Reich, A., an der Heiden, M., Rexroth, U., Hamouda, O., Schneider, J., Veith, T., Mühlemann, B., Wölfel, R., Antwerpen, M., Walter, M., Protzer, U., Liebl, B., Haas, W., Sing, A., Drosten, C., and Zapf, A. (2020). Investigation of a COVID-19 outbreak in Germany resulting from a single travel-associated primary case: a case series. *The Lancet Infectious Diseases*, page S1473309920303145.

Centro National de Epidemiología (2020). Ene-covid-19: Estudio nacional de sero-epidemiología de la infección por sars-cov-2 en españa. Technical report, Instituto de Salud Carlos III.

Du, Z., Xu, X., Wu, Y., Wang, L., Cowling, B. J., and Meyers, L. A. (2020). Serial interval of covid-19 among publicly reported confirmed cases. *Emerg. Infect. Dis.*

Emmenegger, M., Cecco, E. D., Lamparter, D., Jacquat, R. P. B., Ebner, D., Schneider, M. M., Morales, I. C., Schneider, D., Dogancay, B., Guo, J., Wiedmer, A., Domange, J., Imeri, M., Moos, R., Zografou, C., Trevisan, C., Gonzalez-Guerra, A., Carrella, A., Dubach, I. L., Althaus, C. L., Xu, C. K., Meisl, G., Kosmoliaptsis, V., Malinauskas, T., Burgess-Brown, N., Owens, R.,

Mongkolsapaya, J., Hatch, S., Screaton, G. R., Schubert, K., Huck, J. D., Liu, F., Pojer, F., Lau, K., Hacker, D., Probst-Mueller, E., Cervia, C., Nilsson, J., Boyman, O., Saleh, L., Spanaus, K., Eckardstein, A. v., Schaer, D. J., Ban, N., Tsai, C.-J., Marino, J., Schertler, G. F. X., Ebert, N., Thiel, V., Gottschalk, J., Frey, B. M., Reimann, R., Hornemann, S., Ring, A. M., Knowles, T. P. J., Xenarios, I., Stuart, D. I., and Aguzzi, A. (2020). Early peak and rapid decline of SARS-CoV-2 seroprevalence in a Swiss metropolitan region. *medRxiv*, page 2020.05.31.20118554. Publisher: Cold Spring Harbor Laboratory Press.

Flaxman, S., Mishra, S., Gandy, A., Unwin, H., Coupland, H., Mellan, T., Zhu, H., Berah, T., Eaton, J., Perez Guzman, P., Schmit, N., Cilloni, L., Ainslie, K., Baguelin, M., Blake, I., Boonyasiri, A., Boyd, O., Cattarino, L., Ciavarella, C., Cooper, L., Cucunuba Perez, Z., Cuomo-Dannenburg, G., Dighe, A., Djaafara, A., Dorigatti, I., Van Elsland, S., Fitzjohn, R., Fu, H., Gaythorpe, K., Geidelberg, L., Grassly, N., Green, W., Hallett, T., Hamlet, A., Hinsley, W., Jeffrey, B., Jorgensen, D., Knock, E., Laydon, D., Nedjati Gilani, G., Nouvellet, P., Parag, K., Siveroni, I., Thompson, H., Verity, R., Volz, E., Walters, C., Wang, H., Wang, Y., Watson, O., Winskill, P., Xi, X., Whittaker, C., Walker, P., Ghani, A., Donnelly, C., Riley, S., Okell, L., Vollmer, M., Ferguson, N., and Bhatt, S. (2020). Report 13: Estimating the number of infections and the impact of non-pharmaceutical interventions on COVID-19 in 11 European countries. Technical report, Imperial College London.

Grewelle, R. and De Leo, G. (2020). Estimating the Global Infection Fatality Rate of COVID-19. preprint, Infectious Diseases (except HIV/AIDS).

Guan, W.-j., Ni, Z.-y., Hu, Y., Liang, W.-h., Ou, C.-q., He, J.-x., Liu, L., Shan, H., Lei, C.-l., Hui, D. S., Du, B., Li, L.-j., Zeng, G., Yuen, K.-Y., Chen, R.-c., Tang, C.-l., Wang, T., Chen, P.-y., Xiang, J., Li, S.-y., Wang, J.-l., Liang, Z.-j., Peng, Y.-x., Wei, L., Liu, Y., Hu, Y.-h., Peng, P., Wang, J.-m., Liu, J.-y., Chen, Z., Li, G., Zheng, Z.-j., Qiu, S.-q., Luo, J., Ye, C.-j., Zhu, S.-y., and Zhong, N.-s. (2020). Clinical characteristics of coronavirus disease 2019 in china. *New England Journal of Medicine*, 382(18):1708–1720.

Hauser, A., Counotte, M. J., Margossian, C. C., Konstantinoudis, G., Low, N., Althaus, C. L., and Riou, J. (2020). Estimation of SARS-CoV-2 mortality during the early stages of an epidemic: A modeling study in Hubei, China, and six regions in Europe. *PLOS Medicine*, 17(7):e1003189. Publisher: Public Library of Science.

He, X., Lau, E. H. Y., Wu, P., Deng, X., Wang, J., Hao, X., Lau, Y. C., Wong, J. Y., Guan, Y., Tan, X., Mo, X., Chen, Y., Liao, B., Chen, W., Hu, F., Zhang, Q., Zhong, M., Wu, Y., Zhao, L., Zhang, F., Cowling, B. J., Li, F., and Leung, G. M. (2020). Temporal dynamics in viral shedding and transmissibility of COVID-19. *Nature Medicine*, 26(5):672–675.

Hu, Z., Song, C., Xu, C., Jin, G., Chen, Y., Xu, X., Ma, H., Chen, W., Lin, Y., Zheng, Y., et al. (2020). Clinical characteristics of 24 asymptomatic infections

with covid-19 screened among close contacts in nanjing, china. *Science China Life Sciences*, pages 1–6.

Imperial College COVID-19 Response Team, Flaxman, S., Mishra, S., Gandy, A., Unwin, H. J. T., Mellan, T. A., Coupland, H., Whittaker, C., Zhu, H., Berah, T., Eaton, J. W., Monod, M., Ghani, A. C., Donnelly, C. A., Riley, S. M., Vollmer, M. A. C., Ferguson, N. M., Okell, L. C., and Bhatt, S. (2020). Estimating the effects of non-pharmaceutical interventions on COVID-19 in Europe. *Nature*.

ISTAT (2020). Primi risultati dell'indagine di sieroprevalenza sul SARS-CoV-2.

Kanzawa, M., Spindler, H., Anglemyer, A., and Rutherford, G. W. (2020). Will Coronavirus Disease 2019 Become Seasonal? *The Journal of Infectious Diseases*, 222(5):719–721.

Kim, Jasmine, N. H.-D. (2020). Antibody testing shows coronavirus is still spreading in low-income, minority communities in NYC, Gov. Cuomo says. Library Catalog: www.cnbc.com Section: Health & Science.

Kissler, S. M., Tedijanto, C., Goldstein, E., Grad, Y. H., and Lipsitch, M. (2020). Projecting the transmission dynamics of sars-cov-2 through the postpandemic period. *Science*, 368(6493):860–868.

Lauer, S. A., Grantz, K. H., Bi, Q., Jones, F. K., Zheng, Q., Meredith, H. R., Azman, A. S., Reich, N. G., and Lessler, J. (2020). The Incubation Period of Coronavirus Disease 2019 (COVID-19) From Publicly Reported Confirmed Cases: Estimation and Application. *Annals of Internal Medicine*, 172(9):577–582.

Lavezzo, E., Franchin, E., Ciavarella, C., Cuomo-Dannenburg, G., Barzon, L., Del Vecchio, C., Rossi, L., Manganelli, R., Loregian, A., Navarin, N., et al. (2020). Suppression of a sars-cov-2 outbreak in the italian municipality of vo'. *medRxiv*.

Liu, Y., Gayle, A. A., Wilder-Smith, A., and Rocklöv, J. (2020). The reproductive number of COVID-19 is higher compared to SARS coronavirus. *Journal of Travel Medicine*, 27(2):taaa021.

Ma, J. (2020). Estimating epidemic exponential growth rate and basic reproduction number. *Infectious Disease Modelling*, 5:129–141.

Martcheva, M. (2015). *An Introduction to Mathematical Epidemiology*, volume 61 of *Texts in Applied Mathematics*. Springer US, Boston, MA.

Meyerowitz-Katz, G. and Merone, L. (2020). A systematic review and meta-analysis of published research data on covid-19 infection-fatality rates. *medRxiv*.

MISAN (2020). Situación en españa: Enfermedad por el coronavirus (covid-19), 18.5. 2020. Technical report, Ministerio de Sanidad, Centro de Coordinación de Alertas y Emergencias Sanitaria.

Mizumoto, K., Kagaya, K., Zarebski, A., and Chowell, G. (2020). Estimating the asymptomatic proportion of coronavirus disease 2019 (COVID-19) cases on board the Diamond Princess cruise ship, Yokohama, Japan, 2020. *Eurosurveillance*, 25(10).

Modi, C., Boehm, V., Ferraro, S., Stein, G., and Seljak, U. (2020). How deadly is COVID-19? A rigorous analysis of excess mortality and age-dependent fatality rates in Italy. preprint, Epidemiology.

Monto, A. S., DeJonge, P., Callear, A. P., Bazzi, L. A., Capriola, S., Malosh, R. E., Martin, E. T., and Petrie, J. G. (2020). Coronavirus occurrence and transmission over 8 years in the hive cohort of households in michigan. *The Journal of infectious diseases*.

Moriyama, M., Hugentobler, W. J., and Iwasaki, A. (2020). Seasonality of respiratory viral infections. *Annual review of virology*, 7.

New York Health Dep. (2020). COVID-19: Data Summary - NYC Health.

Noll, N. B., Aksamentov, I., Druelle, V., Badenhorst, A., Ronzani, B., Jefferies, G., Albert, J., and Neher, R. (2020). COVID-19 Scenarios: an interactive tool to explore the spread and associated morbidity and mortality of SARS-CoV-2. *medRxiv*, page 2020.05.05.20091363. Publisher: Cold Spring Harbor Laboratory Press.

Ogris, G., Oberhuber, F., Baumegger, D., Moser, W., Schenk, K., and Hofinger, C. (2020). Spread of SARS-CoV-2 in Austria - PCR tests in a representative sample Study report. Technical report, SORA Institute for Social Research and Consulting, Bennogasse 8/2/16, 1080 Vienna, Austria, office@sora.at, Vienna.

Park, M., Cook, A. R., Lim, J. T., Sun, Y., and Dickens, B. L. (2020). A systematic review of covid-19 epidemiology based on current evidence. *Journal of Clinical Medicine*, 9(4):967.

Pastor-Barriuso, R., Perez-Gomez, B., Hernan, M. A., Perez-Olmeda, M., Yotti, R., Oteo, J., Sanmartin, J. L., Leon-Gomez, I., Fernandez-Garcia, A., Fernandez-Navarro, P., Cruz, I., Martin, M., Delgado-Sanz, C., Larrea, N. F. d., Paniagua, J. L., Munoz-Montalvo, J. F., Blanco, F., Larrauri, A., Pollan, M., and Pollan, M. (2020). SARS-CoV-2 infection fatality risk in a nationwide seroepidemiological study. *medRxiv*, page 2020.08.06.20169722. Publisher: Cold Spring Harbor Laboratory Press.

Perez-Saez, J., Lauer, S. A., Kaiser, L., Regard, S., Delaporte, E., Guessous, I., Stringhini, S., Azman, A. S., Alioucha, D., Arm-Vernez, I., Bahta, S., Barbolini, J., Baysson, H., Butzberger, R., Cattani, S., Chappuis, F., Chiovini,

A., Collombet, P., Courvoisier, D., Ridder, D. D., Weck, E. D., D'ippolito, P., Daeniker, A., Desvachez, O., Dibner, Y., Dubas, C., Duc, J., Eckerle, I., Eelbode, C., Merjani, N. E., Emery, B., Favre, B., Flahault, A., Francioli, N., Gétaz, L., Gilson, A., Gonul, A., Guérin, J., Hassar, L., Hepner, A., Hovagemyan, F., Hurst, S., Keiser, O., Kir, M., Lamour, G., Lescuyer, P., Lombard, F., Mach, A., Malim, Y., Marchetti, E., Marcus, K., Maret, S., Martinez, C., Massiha, K., Mathey-Doret, V., Mattera, L., Matute, P., Maugey, J.-M., Meyer, B., Membrez, T., Michel, N., Mitrovic, A., Mohbat, E. M., Nehme, M., Noël, N., Oulevey, H.-K., Pardo, F., Pennacchio, F., Petrovic, D., Picazio, A., Piumatti, G., Pittet, D., Portier, J., Poulain, G., Posfay-Barbe, K., Pradeau, J.-F., Pugin, C., Rakotomiaramanana, R. B., Richard, A., Fine, C. R., Sakvarelidze, I., Salzmann-Bellard, L., Schellongova, M., Schrempft, S., Miranda, M. S., Stimec, M., Tacchino, M., Theurillat, S., Tomasini, M., Toruslu, K.-G., Tounsi, N., Trono, D., Vincent, N., Violot, G., Vuilleumier, N., Waldmann, Z., Welker, S., Will, M., Wisniak, A., Yerly, S., Zaballa, M.-E., and Valle, A. Z. (2020). Serology-informed estimates of SARS-CoV-2 infection fatality risk in Geneva, Switzerland. *The Lancet Infectious Diseases*, 0(0). Publisher: Elsevier.

Richter, L., Schmid, D., Chakeri, A., Maritschnik, S., Pfeiffer, S., and Stadlober, E. (2020). Schätzung des seriellen intervalles von covid19, Österreich. Technical report, Abteilung Infektionsepidemiologie und Surveillance, AGES; Institut für Statistik, Technische Universität Graz. https://www.ages.at/en/wissen-aktuell/publikationen/schaetzung-des-seriellen-intervalles-von-covid19-oesterreich/.

Roser, M., Ritchie, H., Ortiz-Ospina, E., and Hasell, J. (2020). Coronavirus Pandemic (COVID-19). *Our World in Data*.

Salje, H., Tran Kiem, C., Lefrancq, N., Courtejoie, N., Bosetti, P., Paireau, J., Andronico, A., Hozé, N., Richet, J., Dubost, C.-L., Le Strat, Y., Lessler, J., Levy-Bruhl, D., Fontanet, A., Opatowski, L., Boelle, P.-Y., and Cauchemez, S. (2020). Estimating the burden of SARS-CoV-2 in France. *Science*, page eabc3517.

Sanche, S., Lin, Y. T., Xu, C., Romero-Severson, E., Hengartner, N., and Ke, R. (2020). High Contagiousness and Rapid Spread of Severe Acute Respiratory Syndrome Coronavirus 2. *Emerging Infectious Diseases*, 26(7).

Schilling, J., Diercke, M., Altmann, D., Haas, W., and Buda, S. (2020). Vorläufige bewertung der krankheitsschwere von covid-19 in deutschland basierend auf übermittelten fällen gemäß infektionsschutzgesetz. *Epidemiologisches Bulletin*, 17:3–9.

Streeck, H., Schulte, B., Kuemmerer, B., Richter, E., Hoeller, T., Fuhrmann, C., Bartok, E., Dolscheid, R., Berger, M., Wessendorf, L., Eschbach-Bludau, M., Kellings, A., Schwaiger, A., Coenen, M., Hoffmann, P., Noethen, M.,

Eis-Huebinger, A.-M., Exner, M., Schmithausen, R., Schmid, M., and Kuemmerer, B. (2020). Infection fatality rate of SARS-CoV-2 infection in a German community with a super-spreading event. preprint, Infectious Diseases (except HIV/AIDS).

Unwin, H., Mishra, S., Bradley, V., Gandy, A., Vollmer, M., Mellan, T., Coupland, H., Ainslie, K., Whittaker, C., Ish-Horowicz, J., Filippi, S., Xi, X., Monod, M., Ratmann, O., Hutchinson, M., Valka, F., Zhu, H., Hawryluk, I., Milton, P., Baguelin, M., Boonyasiri, A., Brazeau, N., Cattarino, L., Charles, G., Cooper, L., Cucunuba Perez, Z., Cuomo-Dannenburg, G., Djaafara, A., Dorigatti, I., Eales, O., Eaton, J., Van Elsland, S., Fitzjohn, R., Gaythorpe, K., Green, W., Hallett, T., Hinsley, W., Imai, N., Jeffrey, B., Knock, E., Laydon, D., Lees, J., Nedjati Gilani, G., Nouvellet, P., Okell, L., Ower, A., Parag, K., Siveroni, I., Thompson, H., Verity, R., Walker, P., Walters, C., Wang, Y., Watson, O., Whittles, L., Ghani, A., Ferguson, N., Riley, S., Donnelly, C., Bhatt, S., and Flaxman, S. (2020). Report 23: State-level tracking of COVID-19 in the United States. Technical report, Imperial College London.

Virtanen, P., Gommers, R., Oliphant, T. E., Haberland, M., Reddy, T., Cournapeau, D., Burovski, E., Peterson, P., Weckesser, W., Bright, J., van der Walt, S. J., Brett, M., Wilson, J., Jarrod Millman, K., Mayorov, N., Nelson, A. R. J., Jones, E., Kern, R., Larson, E., Carey, C., Polat, İ., Feng, Y., Moore, E. W., Vand erPlas, J., Laxalde, D., Perktold, J., Cimrman, R., Henriksen, I., Quintero, E. A., Harris, C. R., Archibald, A. M., Ribeiro, A. H., Pedregosa, F., van Mulbregt, P., and Contributors, S. . . (2020). SciPy 1.0: Fundamental Algorithms for Scientific Computing in Python. *Nature Methods*, 17:261–272.

Ward, H., Atchison, C. J., Whitaker, M., Ainslie, K. E. C., Elliott, J., Okell, L. C., Redd, R., Ashby, D., Donnelly, C. A., Barclay, W., Darzi, A., Cooke, G., Riley, S., and Elliott, P. (2020). Antibody prevalence for SARS-CoV-2 in England following first peak of the pandemic: REACT2 study in 100,000 adults. *medRxiv*, page 2020.08.12.20173690. Publisher: Cold Spring Harbor Laboratory Press.

WHO (2020a). Estimating mortality from COVID-19. https://www.who.int/news-room/commentaries/detail/estimating-mortality-from-covid-19 (2020-08-24).

WHO (2020b). Naming the coronavirus disease (COVID-19) and the virus that causes it. https://www.who.int/emergencies/diseases/novel-coronavirus-2019/technical-guidance/naming-the-coronavirus-disease-(covid-2019)-and-the-virus-that-causes-it (2020-05-29).

Wilson, L. (2020). SARS-CoV-2, COVID-19, Infection Fatality Rate (IFR) Implied by the Serology, Antibody, Testing in New York City. *SSRN Electronic Journal*.

Zhang, W. (2020). Estimating the presymptomatic transmission of COVID19 using incubation period and serial interval data. preprint, Infectious Diseases (except HIV/AIDS).

Zhou, F., Yu, T., Du, R., Fan, G., Liu, Y., Liu, Z., Xiang, J., Wang, Y., Song, B., Gu, X., Guan, L., Wei, Y., Li, H., Wu, X., Xu, J., Tu, S., Zhang, Y., Chen, H., and Cao, B. (2020). Clinical course and risk factors for mortality of adult inpatients with COVID-19 in Wuhan, China: a retrospective cohort study. *The Lancet*, 395(10229):1054–1062.

Zhuang, Z., Zhao, S., Lin, Q., Cao, P., Lou, Y., Yang, L., Yang, S., He, D., and Xiao, L. (2020). Preliminary estimates of the reproduction number of the coronavirus disease (COVID-19) outbreak in Republic of Korea and Italy by 5 March 2020. *International Journal of Infectious Diseases*, 95:308–310.